

# Far-infrared photoresponse of granular $\text{YBa}_{2.1}\text{Cu}_{3.4}\text{O}_{7-x}$

U. Strom, J. C. Culbertson, and S. A. Wolf  
*Naval Research Laboratory, Washington, D.C. 20375-5000*

F. Gao and D. B. Tanner  
*Department of Physics, University of Florida, Gainesville, Florida 32611*

G. L. Carr  
*Grumman Corporate Research Center, Bethpage, New York 11714*  
 (Received 13 March 1992; Revised manuscript received 3 August 1992)

The response of a granular film of  $\text{YBa}_{2.1}\text{Cu}_{3.4}\text{O}_{7-x}$  to pulsed far-infrared light has been measured at temperatures which are near the resistive onset of the film. The photoresponse at  $26.0\text{ cm}^{-1}$  is interpreted due to the direct modulation of intergrain Josephson currents ("current mode") by the incident far-infrared light. The observed dependence on far-infrared power ( $\sim P^{1/2}$ ) is consistent with a superconducting energy gap which is much larger than  $26.0\text{ cm}^{-1}$ . There is evidence for a current mode response at  $87.7$  and  $152\text{ cm}^{-1}$ , but with a greatly reduced photoresponse magnitude. The decrease in photoresponse measured at  $87.7$  and  $152\text{ cm}^{-1}$  is attributed to intergrain capacitive effects.

## I. INTRODUCTION

The investigation of the photoresponse of high-temperature superconducting films is motivated by possible infrared sensor applications and also by interest in exploring the dynamical response of these materials to electromagnetic radiation. The present paper is concerned with granular films having thickness on the order of or less than the magnetic penetration depth. Such a system can be described in terms of a disordered two-dimensional (2D) array of weakly coupled Josephson junctions or weak links.<sup>1,2</sup>

It has been previously shown<sup>3</sup> that visible light (either steady state or pulsed) incident on 2D granular films leads to a resistive increase which is not consistent with a uniform bolometric heating of the film. We consider a model in which an induced flux-flow resistance due to a vortex unbinding or depinning process<sup>3-5</sup> occurs when photons having an energy greater than the superconducting gap are absorbed.

It is possible for photons having energies near and below the superconducting gap to modulate the Josephson current between superconducting grains. The photoresponse is characterized by dependences on intensity and temperature which can vary significantly for photon energies above and below the superconducting energy gap. Recent observations<sup>6</sup> in 2D granular NbN/BN films<sup>7,8</sup> established a crossover from an above- to a below-gap response. Other far-infrared photoresponse measurements have been reported. These include the measurements on PbBi oxide films,<sup>9</sup> granular NbN films,<sup>10</sup> and the recent work<sup>11</sup> on  $\text{Bi}_2\text{Sr}_2\text{CaCuO}_8$ . In particular, the latter measurements report dependences of the far-infrared photoresponse on the intensity of the far-infrared radiation which are in agreement with results reported in the present paper.

The present work extends the far-infrared response

measurements carried out on NbN/BN films<sup>6</sup> to a granular film of  $\text{YBa}_2\text{Cu}_{3.4}\text{O}_{7-x}$  (YBCO). A measurement at  $20\text{ cm}^{-1}$  carried out on a YBCO film deposited on sapphire was reported earlier.<sup>12</sup> We will show that the YBCO film exhibits a far-infrared photoresponse that is qualitatively similar to that of granular NbN/BN, that is, a low-frequency ( $\omega < 4kT_c/\hbar$ ) photoresponse which, compared to the high-frequency response, has a greatly enhanced magnitude and a much weaker temperature dependence. We observe significantly different dependences on the far-infrared light intensity for the two materials, which we will relate to the different magnitudes of their respective superconducting energy gaps.

The outline of the paper is as follows. The relevant experimental details are discussed in Sec. II and the experimental results are presented in Sec. III. The focus here and in the discussion in Sec. IV is on the data taken at the lowest far-infrared frequency ( $26.0\text{ cm}^{-1}$ ) and a comparison of the  $26.0\text{-cm}^{-1}$  data with measurements made at  $87.7$  and  $152\text{ cm}^{-1}$ .

## II. EXPERIMENTAL DETAILS

The YBCO film was prepared by radio-frequency magnetron sputtering onto a MgO substrate and subsequent oxygen annealing. Details of the sample preparation have been described previously.<sup>3</sup> The  $2500\text{-\AA}$ -thick film was slightly copper rich with composition  $\text{YBa}_{2.1}\text{Cu}_{3.4}\text{O}_{7-x}$ . A scanning electron microscopy (SEM) photograph of the film, shown in Fig. 1, reveals an array of irregularly shaped granules of micron and sub-micron size. The film resistance is thermally activated above  $100\text{ K}$  (i.e., decreases with increasing temperature, consistent with intergrain hopping transport in the normal state). The film was scribed and contacted with evaporated Ag pads to allow four-probe transport or two-probe pulsed photoresponse measurements. The width of

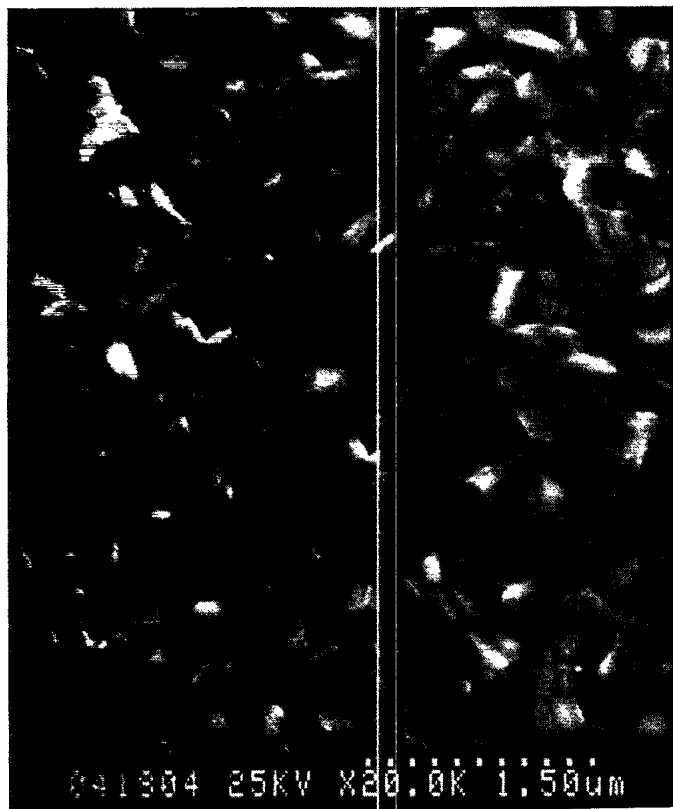


FIG. 1. Scanning electron micrograph of the granular  $\text{YBa}_{2.1}\text{Cu}_{3.4}\text{O}_{7-x}$  film. Crystallites are several tenths to about  $1\ \mu\text{m}$  in size, and are nearly randomly oriented.

the current path was 2 mm.

The far-infrared photoresponse measurements<sup>6</sup> were carried out with a pulsed super-radiant light source which provided 50-ns-long pulses with a maximum energy of  $1\ \mu\text{J}/\text{cm}^2$ -pulse, which is comparable to the maximum energy per pulse for the 10-ns pulsed visible light source. The far-infrared beam diameter was approximately 1 cm. The temperature rise in the film is estimated<sup>3</sup> to be much less than 1 K. The radiation was nearly monochromatic with wavelengths of  $385\ \mu\text{m}$  ( $26.0\ \text{cm}^{-1}$ , 779 GHz, 3.23 meV),  $114\ \mu\text{m}$  ( $87.7\ \text{cm}^{-1}$ , 2.63 THz, 10.90 meV), and  $66.0\ \mu\text{m}$  ( $151.5\ \text{cm}^{-1}$ , 4.55 THz, 18.82 meV). The far-infrared light intensity has been calibrated using a pyroelectric and a fast Ga-doped Ge detector.

Measurements of the far-infrared reflectivity and transmissivity have been obtained for the same film. Details concerning these measurement techniques can be found elsewhere.<sup>13</sup>

### III. EXPERIMENTAL RESULTS

The far-infrared transmittance  $\mathcal{T}$  of the YBCO film attached to the MgO substrate is shown in Fig. 2(a). The dominant feature of the 100- and 300-K spectra is the transmittance onset of MgO below  $80\ \text{cm}^{-1}$ . Multiphonon contributions due to MgO are observed near 100, 155, and  $290\ \text{cm}^{-1}$ . The transmittance spectrum for MgO at 20 K is relatively featureless below  $100\ \text{cm}^{-1}$ . The reflectance  $\mathcal{R}$  of the YBCO/MgO structure is shown

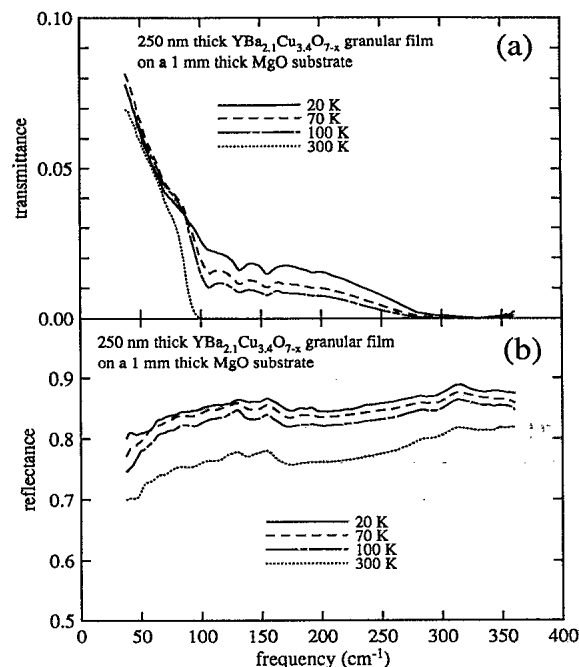


FIG. 2. (a) Reflectance and (b) transmittance as function of temperature of granular YBCO film deposited on a MgO substrate.

in Fig. 2(b). The reflectance is seen to decrease toward lower frequencies, in contrast to observations for high-quality crystals<sup>14</sup> and epitaxially grown films<sup>15</sup> which approach a 100% reflectance below  $100\ \text{cm}^{-1}$ .

The absorbance of the film,  $A = 1 - \mathcal{R} - \mathcal{T}$ , is shown in Fig. 3. The effects of the substrate have been removed as described in Ref. 13. It is seen that the absorbance at a temperature of 20 K is nearly independent of frequency between 50 and  $170\ \text{cm}^{-1}$ . This result will be significant when interpreting the distinctly different dependences of the photoresponse measured as a function of far-infrared frequency in this spectral range.

The granular YBCO film investigated here has a resis-

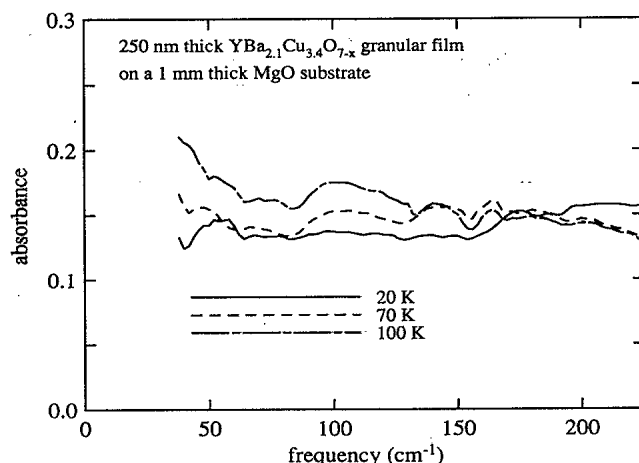


FIG. 3. Absorbance of a YBCO film (same as in Figs. 1 and 2) as a function of temperature. The effect of a MgO substrate has been removed according to method described in Ref. 13.

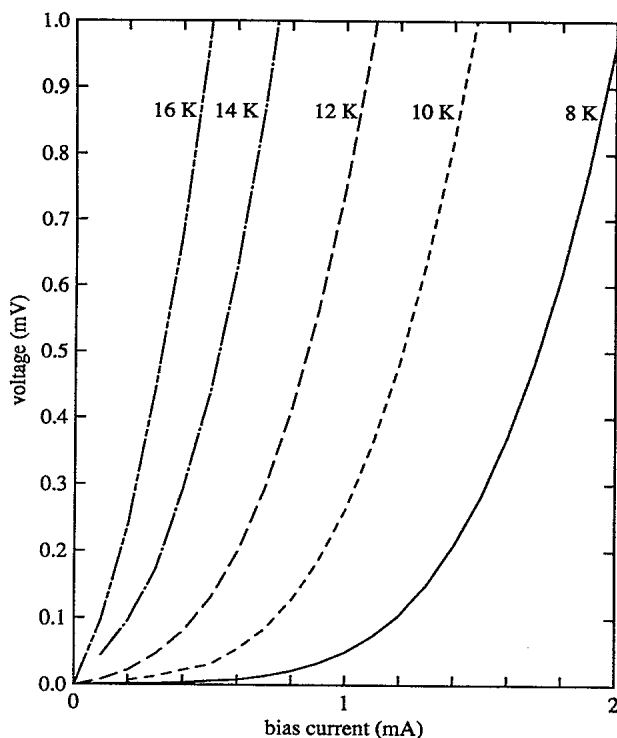


FIG. 4. Current-voltage characteristics of the YBCO film as a function of temperature.

tive onset corresponding to the superconducting transition temperature of the grains at  $T_{cg} = 82$  K. The temperature below which the resistance drops rapidly toward zero is  $T_c \sim 11$  K. The current-voltage relations near  $T_c$  are shown in Fig. 4. These have been previously analyzed and interpreted<sup>3</sup> in terms of a Kosterlitz-Thouless transition with  $T_c \sim T_{KT} \sim 11.2$  K. This interpretation implies that the resistive onset near 11 K is dominated by the thermally induced dissociation of vortex-antivortex pairs.<sup>1-4</sup>

The associated response to pulsed visible light has been shown previously<sup>3</sup> and is reproduced in Fig. 5 to enable comparison with the far-infrared pulsed photoresponse. Noteworthy of the data in Fig. 5 is the nonlinear dependence of the photoresponse amplitude on bias current below 10 K which was shown to be inconsistent with an equilibrium bolometric response.<sup>3</sup> This result is in contrast to the nearly linear dependence on bias current at the highest temperatures ( $>20$  K); in this temperature range the photoresponse is primarily bolometric in nature.

The far-infrared response to  $26.0\text{-cm}^{-1}$  light has been measured for 0.375 and 0.75 mA. The results are shown in Fig. 6. Below 15 K the response to  $26\text{-cm}^{-1}$  light varied less with temperature than did the response to visible light using the same bias current. This same qualitative trend was also observed for NbN/BN measured at the same far-infrared frequency.<sup>6</sup>

In Figs. 7(a)–7(c) are shown the  $26.0\text{-cm}^{-1}$  photoresponse measurements as a function of bias current for three temperatures (5, 11, and 20 K). The dots represent the photoresponse integrated from 0 to 50 ns, and the squares represent the response integrated between 70 and

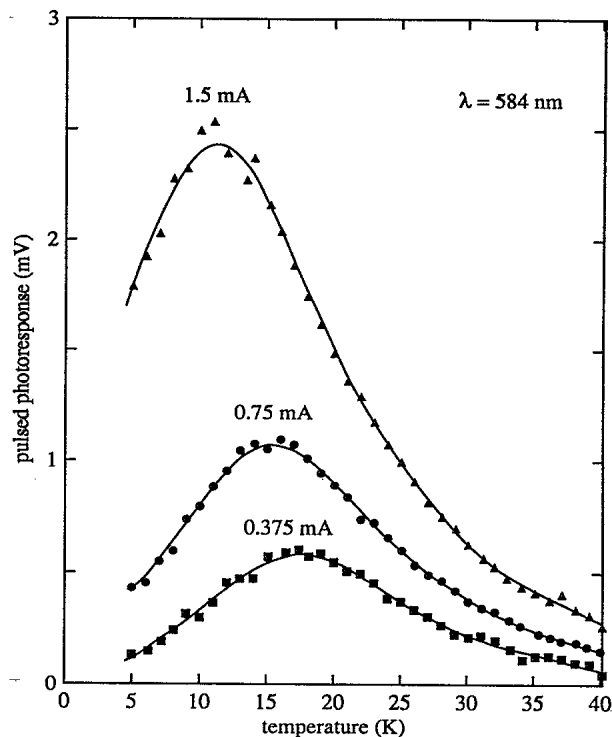


FIG. 5. Photoresponse of film to pulsed visible (584-nm) radiation ( $\sim 10$ -ns pulse duration) for different bias currents. This figure is the same as published in Ref. 3 (Fig. 10).

100 ns. The “slower” contribution has a well-defined current onset, especially at the lower temperatures. The magnitude of the onset is near 1.5 mA at 5 K, 0.6 mA at 11 K, and zero mA at 20 K. The photoresponse depends

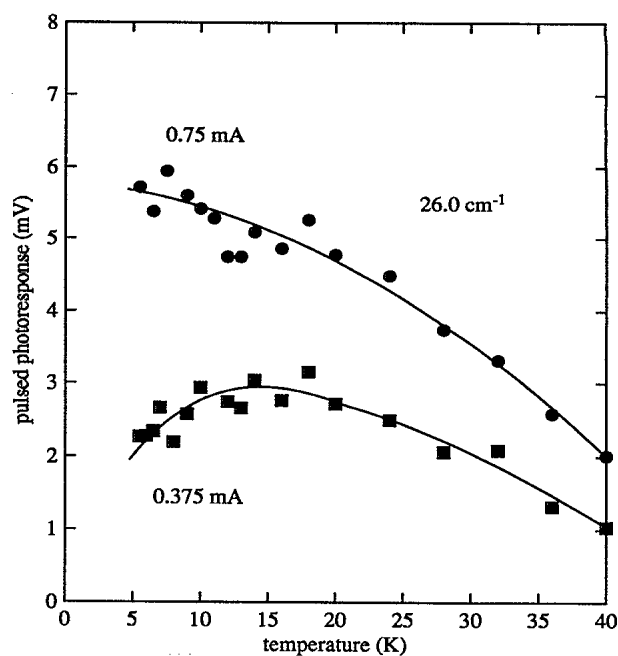


FIG. 6. Response of a YBCO film to a  $26.0\text{-cm}^{-1}$  pulsed photoresponse ( $\sim 50$ -ns pulse duration) as a function of temperature for two different bias currents. Incident peak power level  $\sim 0.2$  W/cm<sup>2</sup>.

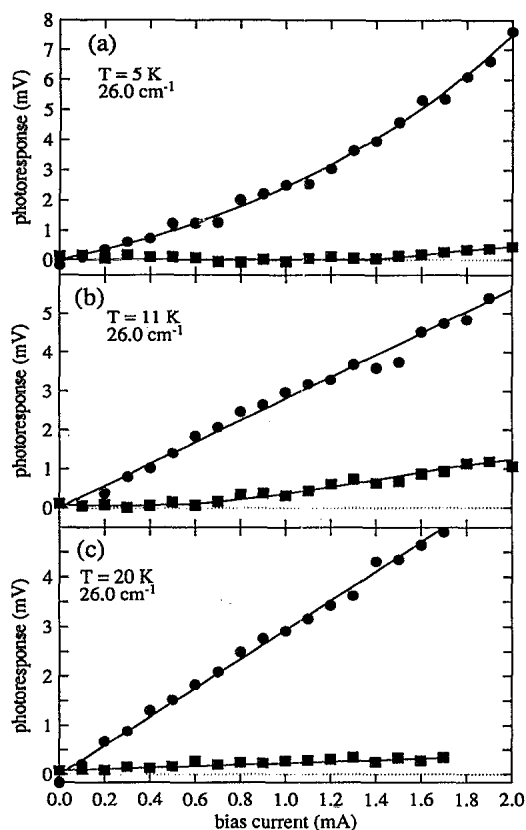


FIG. 7. Response of a YBCO film to  $26.0\text{-cm}^{-1}$  pulsed radiation as a function of bias currents and temperature. Dots, integrated photoresponse from 0 to 50 ns; squares, integrated photoresponse from 70 to 100 ns. Incident peak power level  $\sim 0.1 \text{ W/cm}^2$ .

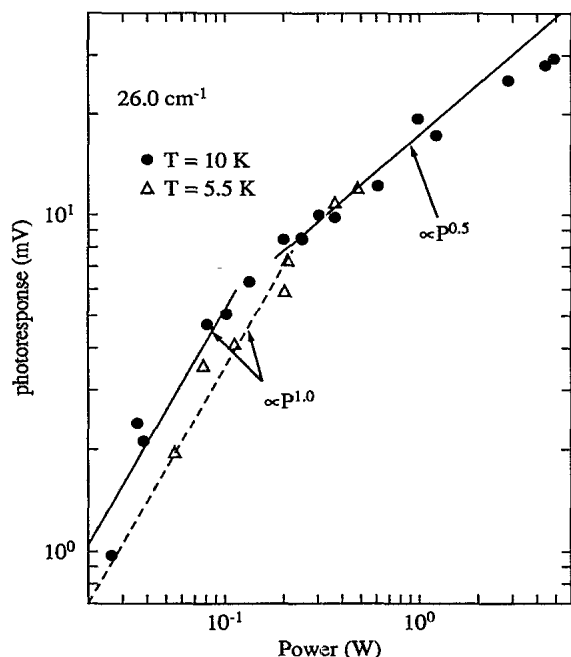


FIG. 8. Response of a YBCO film to a  $26.0\text{-cm}^{-1}$  pulsed radiation as a function of incident far-infrared power for two temperatures. Bias current is  $1.5 \text{ mA}$ .

nonlinearly on bias current for  $T = 5 \text{ K}$ , but is linearly dependent on bias current for  $T \geq 11 \text{ K}$ . The magnitude of the photoresponse depends on the intensity of the far-infrared radiation. In Fig. 8 are shown results at  $26.0 \text{ cm}^{-1}$  for two different temperatures. The response is linearly proportional to the far-infrared power  $P$  for sufficiently low power levels. A gradual turnover to a lower power dependence is observed near  $0.1 \text{ W}$  at  $10 \text{ K}$ , and  $0.2 \text{ W}$  at  $5 \text{ K}$ .

Photoresponse measurements carried out at  $152 \text{ cm}^{-1}$  are shown in Fig. 9. Comparison of these results with analogous measurements at  $584 \text{ nm}$  (Fig. 5) reveals that the  $152\text{-cm}^{-1}$  response curves are characterized by the same strong temperature dependence observed for visible light, but with the maxima in the photoresponse shifted to lower temperatures. Comparison of the  $152\text{-cm}^{-1}$  results with the  $26.0\text{-cm}^{-1}$  data (Fig. 6), demonstrates that the direct modulation of Josephson currents is considerably reduced at the higher frequency.

The measurements carried out at  $87.7 \text{ cm}^{-1}$ , together with the  $26.0\text{-cm}^{-1}$  and visible light data, are shown in Fig. 10. Smooth curves have been drawn through the data instead of showing data points in order to facilitate comparison between the  $87.7$ ,  $26.0\text{-cm}^{-1}$ , and visible light response. Noteworthy are the significant changes with bias current for the  $87.7\text{-cm}^{-1}$  response below  $10 \text{ K}$ . The  $26.0\text{-cm}^{-1}$  and visible photoresponse data shown in Fig. 10 have been normalized to the  $87.7\text{-cm}^{-1}$  data near their respective peak amplitudes.

The power dependences of the response to  $152\text{-}$  and to  $26\text{-cm}^{-1}$  radiation are shown in Fig. 11. The  $152\text{-cm}^{-1}$  light response is linear in power below  $10 \text{ W}$  of incident power. Moreover, the responsivity of the film is much lower at  $152 \text{ cm}^{-1}$ . This result is in sharp contrast to the  $P^{0.5}$  dependence observed for power levels as low as  $0.2$

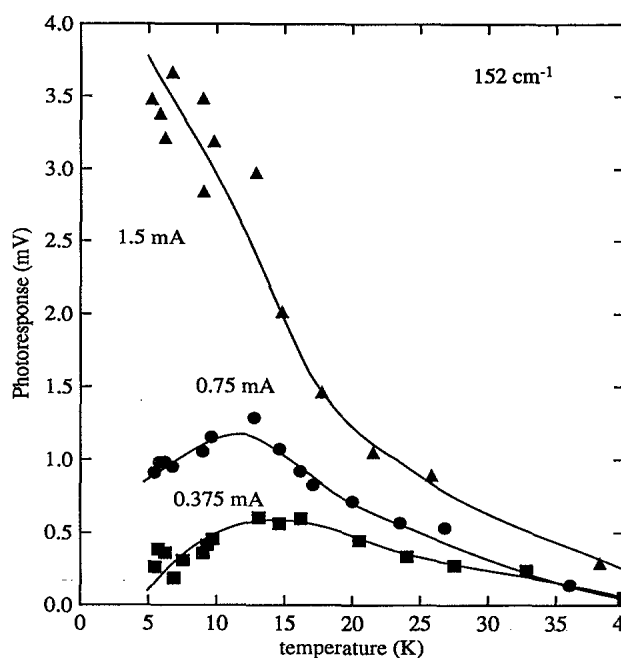


FIG. 9. Response of a YBCO film to a  $152\text{-cm}^{-1}$  pulsed radiation as a function of bias current and temperature.

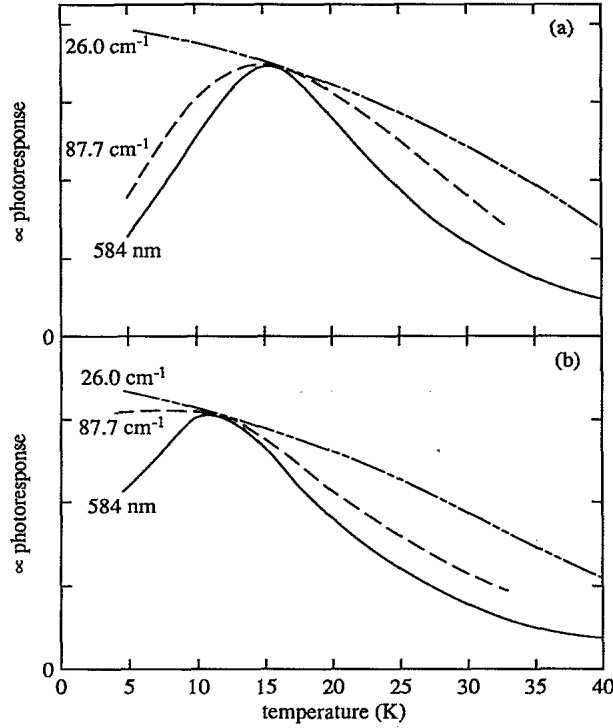


FIG. 10. Comparison of the normalized photoresponse of the YBCO film at two far-infrared energies and for visible light. (a) Bias current 0.75 mA; (b) bias current 1.5 mA.

W at  $26.0 \text{ cm}^{-1}$ . The deviation from the  $P^{0.5}$  dependence in Fig. 11 at the highest power levels ( $> 2 \text{ W}$ ) is likely due to heating effects. The onset of the saturation coincides with the appearance of a long-time tail for the time-

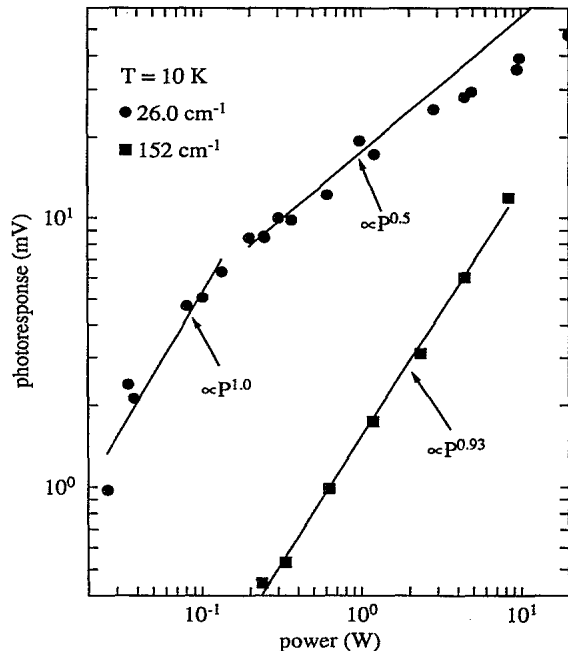


FIG. 11. Comparison of 26.0- and 152- $\text{cm}^{-1}$  photoresponse as a function of incident far-infrared power. The bias current is 1.5 mA.

resolved response for  $P > 2 \text{ W}$ . We note that the observed  $P^{1/2}$  dependence is in agreement with the intensity measurements of the  $20.2\text{-cm}^{-1}$  photoresponse reported recently<sup>11</sup> for  $\text{Bi}_2\text{Sr}_2\text{CaCuO}_8$  films.

#### IV. DISCUSSION

Data have been presented for the response of a granular YBCO film to pulsed far-infrared light at 26.0, 87.7, and  $152 \text{ cm}^{-1}$ . In the next section we discuss the expected dependences of the photoresponse on radiation power and bias current within the resistively shunted junction (RSJ) model and consider the  $26.0\text{-cm}^{-1}$  results as evidence that far-infrared radiation directly modulates currents across superconductive weak links.

##### A. Photoresponse at $26.0 \text{ cm}^{-1}$

The important features of the  $26.0\text{-cm}^{-1}$  data (Fig. 11) are its square law ( $\sim P$ ) response for low far-infrared power ( $\leq 0.1 \text{ W}$ ), and its weaker power dependence ( $\sim P^{0.5}$ ) at higher incident power levels ( $> 0.1 \text{ W}$ ). In addition, for temperatures near and above  $T_c$  ( $\sim 11 \text{ K}$ ) the photoresponse (with  $P > 0.1 \text{ W}$ ) is proportional to the bias current  $I_b$  (see Fig. 7).

Nearly identical observations to those outlined above were made by Bertin and Rose<sup>16</sup> who investigated the response of granular Sn films to microwave radiation (9–35 GHz). These authors modeled their results with the following form for the induced voltage:<sup>16</sup>

$$\delta V = I(\delta R / \delta T) \delta T + (\delta V / \delta I) \delta I, \quad (1)$$

where the first term is due to the bolometric response of the film. The second term, referred to as the “current mode,” was subsequently identified with the response to microwave radiation of a disordered array of Josephson junctions or weak links. The current mode can be modeled in various ways. A simple approach, suggested by Bertin and Rose,<sup>17</sup> is to approximate the nonlinear current-voltage curves in terms of a series expansion of the total current

$$I = I_b + i(t), \quad (2)$$

where  $I_b$  is the bias current and  $i(t)$  is the current induced by the microwave radiation. In the present experiment  $i(t)$  is induced by a periodic pulse of monochromatic radiation, so that

$$\begin{aligned} i(t) &= i_0, & 0 < t < 50 \text{ ns} \\ i(t) &= 0, & t > 50 \text{ ns} \end{aligned} \quad (3)$$

with a repetition rate of  $\sim 0.5 \text{ Hz}$ . Bertin and Rose approximated the current-voltage curves in terms of a power series expansion of the total current  $I$  and derived the following dependence of the photoresponse in the “large” and “small” signal limits:<sup>17</sup>

$$\delta V \propto I_b, \quad i_0 \gg I_b, \quad (4)$$

$$\delta V \propto P, \quad i_0 \ll I_b. \quad (5)$$

A  $P^{1/2}$  power dependence was deduced for the special

large signal case where  $i_0 \gg |I_b - I_c|$ :

$$\delta V \propto P^{1/2}, \quad i_0 \gg |I_b - I_c|, \quad (6)$$

where  $I_c$  is the critical current. Our experimental observations at  $26.0 \text{ cm}^{-1}$  shown in Figs. 7 and 11 are accurately described by Eqs. (4)–(6).

Equations (5) and (6) are also predicted by the resistively shunted junction model for the case of a single Josephson junction in the presence of high-frequency radiation.<sup>18</sup> This model has been shown to be useful for the description of regular Josephson junction arrays<sup>19,20</sup> and more recently also for disordered arrays.<sup>21</sup> Regular arrays typically exhibit<sup>20,21</sup> giant Shapiro steps at large multiples of the single Josephson value  $\hbar v/2e$ . Giant steplike features in the  $I$ - $V$  characteristics have also been observed for granular superconductors.<sup>22</sup> It is instructive to compare the general dependence on far-infrared light intensity shown in Fig. 11 with the prediction of the RSJ model.

The RSJ model response depends sensitively on the magnitude of the parameter  $\Omega \equiv \hbar\omega/2eI_cR$ , where  $I_c$  is the critical current.<sup>18</sup> For low capacitance junctions, the  $I_cR$  product can achieve its maximum value  $\pi\Delta/2e$ , so that  $\Omega = \hbar\omega/\pi\Delta$ . For  $\Omega \geq 1$ , the dependence of the zero voltage Josephson step on light intensity is close to that of a Bessel function, which results in a square law response ( $\propto P$ ) for low power levels.<sup>18</sup> At higher power levels the magnitude of the photoresponse oscillates as a function of far-infrared radiation intensity. These oscillations are expected to be broadened by disorder to yield a weak dependence of the magnitude of the photoresponse on far-infrared radiation power. This prediction is consistent with the  $P^\alpha$ ,  $\alpha \sim 0.12$ , dependence observed<sup>6</sup> in a NbN/BN cermet at  $26.0 \text{ cm}^{-1}$ . At this frequency  $\Omega \sim 0.5$ , given  $2\Delta(\text{NbN}) = 35 \text{ cm}^{-1}$ , and the sample marginally satisfies the requirement for a Bessel functionlike response.<sup>6,18</sup> For  $\Omega \ll 1$ , the RSJ model predicts a distinctly non-Bessel functionlike response,<sup>18</sup> which is  $\propto P$  at low power levels and  $\propto P^{1/2}$  at higher power levels. For example, for  $\Omega = 0.1$  the  $P^{1/2}$  dependence extends over at least one order of magnitude above the power level which defines the transition from a  $P$  to a  $P^{1/2}$  dependence. For 10-GHz radiation and Sn films ( $2\Delta \sim 15 \text{ cm}^{-1}$ ),  $\Omega = 2 \times 10^{-3}$  and the  $P^{1/2}$  dependence is expected to dominate the microwave power dependence. This prediction is corroborated by experiments of Bertin and Rose<sup>17</sup> on granular Sn films who observed a  $P^{1/2}$  dependence over four orders of magnitude in microwave power. Based on these arguments it can be concluded that the present power dependence data obtained for YBCO at  $26.0 \text{ cm}^{-1}$  is consistent with the condition  $\Omega \ll 1$ .

A further test of the above model is to relate the transition from a small to a large signal response to the magnitude of  $i_0 \equiv i_{0c}$  near this transition. From Eqs. (4) and (6) it follows that  $i_{0c} \sim I_b \sim I_c$ . We want to relate the magnitude of  $I_c \sim 1 \text{ mA}$  to the induced current  $i_0 = i_{0c}$  appropriate for the transition from a  $P$  to a  $P^{1/2}$  dependence. According to Fig. 11 the transition from a  $P$  to a  $P^{1/2}$  dependence occurs for an incident power level of

$\sim 0.1 \text{ W}$ . This is the power level incident on the outer window of the Dewar. The power incident on the effective sample area is estimated to be  $0.01 \text{ W}$ . The actual absorbed power in the film is about 10% of the incident power, or  $0.001 \text{ W}$ , because of the finite absorptivity of the film ( $\sim 13\%$  according to Fig. 3). The induced current  $i_0$  is obtained by equating  $P_{\text{abs}} = i_0^2 R_f$ , where  $R_f$  is the far-infrared impedance of the film. The film impedance can be estimated from the transmittance and absorbance to be  $R_f \sim Z_0(T/A) \sim 120\Omega$ , which is close to the actual normal-state resistance of the film  $R_n \sim 150\Omega$ . This yields  $i_0 = 2 \text{ mA}$ , which is larger than the estimate of  $i_0 \sim 1 \text{ mA}$ . The above estimate must be considered rather approximate, but it does indicate that the current mode model predicts the correct order of magnitude of the induced high-frequency current in the granular film.

There are, in addition to dependences on power and current discussed above, important differences between the temperature dependences of the  $26.0\text{-cm}^{-1}$  and visible light ( $584\text{-nm}$ ) data. The  $584\text{-nm}$  data show a peak corresponding to the onset in resistance near  $T \sim T_c$ . By contrast, at  $26.0 \text{ cm}^{-1}$ , for bias currents of  $0.75$  and  $1.5 \text{ mA}$ , there is no evidence of a photoresponse peak near  $T_c$ . The induced current  $i(t)$  dominates, as in Eq. (2), the thermally induced depairing processes near  $T_c$ . The temperature dependence of the photoresponse is now dominated by processes approaching  $T_{c0} \sim 82 \text{ K}$ . At sufficiently low bias currents (such as for the  $0.375\text{-mA}$  data shown in Fig. 6) thermal depairing again becomes important at the lowest temperatures, even though the direct process outlined by Eqs. (2)–(6) is still applicable.

### B. Photoresponse at $87.7$ and $152 \text{ cm}^{-1}$

Inspection of Fig. 11 reveals that the photoresponse at  $152 \text{ cm}^{-1}$  is proportional to the far-infrared power throughout the investigated power range. In addition, the coefficient of the  $\propto P$  photoresponse at  $152 \text{ cm}^{-1}$  is a factor of  $\sim 25$  smaller compared to the  $\propto P$  response at  $26.0 \text{ cm}^{-1}$ . (Note the  $87.7\text{-cm}^{-1}$  response is also  $\propto P$  and its magnitude is comparable to that measured at  $152 \text{ cm}^{-1}$  within our factor of two experimental uncertainty of determining an absolute measure of the far-infrared photoresponse.) Within the framework of the RSJ model, the loss in photoresponse amplitude at the higher far-infrared frequencies implies that most of the far-infrared light-induced current is shunted through paths other than the inductive Josephson elements,<sup>16</sup> moving a transition from a  $P$  to  $P^{1/2}$  response to higher power levels than shown in Fig. 11.

In addition to the  $\propto P$  dependence and the reduced intensity relative to  $26.0 \text{ cm}^{-1}$ , the  $87.7\text{-cm}^{-1}$  response at low temperatures ( $< 10 \text{ K}$ ) exhibits a transition from a temperature-dependent to a nearly temperature-independent response as the bias current is increased from  $0.75$  to  $1.5 \text{ mA}$  (see Fig. 10). This observation supports the existence of direct coupling to Josephson junctions or weak links by the  $87.7\text{-cm}^{-1}$  radiation, albeit with reduced magnitude relative to  $26.0 \text{ cm}^{-1}$ .

There is no comparable evidence for direct coupling at  $152 \text{ cm}^{-1}$ . In fact, the photoresponse for  $T > 15 \text{ K}$  has

the same dependence on current and temperature as is observed for 584-nm light (Fig. 5). However, inspection of Fig. 9 shows that the  $152\text{-cm}^{-1}$  photoresponse peaks at considerably lower temperatures for a given bias current than seen for the 584-nm light. A possible explanation is that the effective current in the film is increased by the incident  $152\text{-cm}^{-1}$  radiation in a manner analogous to Eq. (2), but essentially all of the induced current within the framework of the RSJ model is shunted through the noninductive elements of the effective circuit. The above explanation requires that the temperature dependence of the photoresponse will depend on the intensity of the pulsed far-infrared radiation. This has been observed with a shift of the normalized photoresponse to lower temperatures with increasing pump power.

### C. The superconducting energy gap

Various techniques have been used in attempts to obtain information about the superconducting energy gap in  $\text{YBa}_2\text{Cu}_3\text{O}_7$ . Measurements have been performed on oriented thin films and single crystals. Features in the Raman scattering,<sup>23</sup> tunneling,<sup>24</sup> and infrared reflectivity<sup>25</sup> data have been interpreted as gaplike features in the  $200\text{--}500\text{-cm}^{-1}$  range, although the features are not consistent with a BCS-like interpretation. Kamaras *et al.*<sup>15</sup> have pointed out that the features observed in the above spectral range in IR reflectivity should not be assigned to a superconducting gap. They argue that, in the clean limit, which is appropriate for these materials, the superconducting gap cannot be easily determined by infrared absorption. Reflectivity data on single crystals have been interpreted<sup>25</sup> in terms of an optical gap near  $500\text{-cm}^{-1}$ . These results, however, are not entirely in accord with calorimetric absorption measurements,<sup>26</sup> carried out below  $400\text{-cm}^{-1}$ .

Tunneling measurements<sup>24</sup> carried out on single-crystal  $\text{YBa}_2\text{Cu}_3\text{O}_7$  show structure near  $4\text{ meV}$  ( $\sim 32\text{-cm}^{-1}$ ),  $19\text{ meV}$  ( $153\text{-cm}^{-1}$ ), and  $36\text{ meV}$  ( $\sim 290\text{-cm}^{-1}$ ). A multigap system has also been proposed on the basis of Raman scattering,<sup>23</sup> although the energies of the Raman features differ from those observed by tunneling measurements. A recent measurement<sup>27</sup> of the temperature dependence of the magnetic penetration depth in  $\text{YBa}_2\text{Cu}_3\text{O}_{7-x}$  films can be interpreted in terms of two gaps  $2\Delta_1 \sim 17.5\text{ meV}$  and  $2\Delta_2 \sim 30.5\text{ meV}$ . According to an alternative explanation,<sup>27</sup> the smaller gap is interpreted as a reduced weak-link gap  $2\Delta^* \sim 12\text{--}14\text{ meV}$ . A two-gap interpretation has been proposed by Kresin and Wolf<sup>28</sup> on the basis of a Fermi-liquid multiband model. A treatment by Press and Jha<sup>29</sup> has considered an anisotropic gap and an open Fermi surface, which, when fit to existing optical data, leads to a proposal of two gaps differing by a factor of 3–4. Within the interpretation of Kresin and Wolf, the smaller gap  $2\Delta_1$  depends sensitively on the coupling between carriers associated with the copper-oxide planes and those carriers associated with the copper-oxide chains. Structural and stoichiometric disorder, which will tend to reduce  $2\Delta_1$ , is predicted to have much less effect on reducing  $T_{c0}$ . For our film,  $T_{c0} \sim 82\text{ K}$  is rela-

tively large, considering the significant deviation from stoichiometry ( $\sim 10\%$  Cu excess) and the large intergrain disorder, leading to a thermally activated hopping conductivity for  $T > T_{c0}$ . Thus, we can expect that the  $2\Delta_1$  gap, if it exists, is not well defined for our granular film. This prediction agrees with the observed power dependence of the  $26.0\text{-cm}^{-1}$  photoresponse, which was interpreted in terms of the condition  $\Omega \ll 1$ , i.e.,  $\hbar\omega \ll 2\Delta$ , and therefore  $2\Delta \sim 2\Delta_2 \gg 26\text{ cm}^{-1}$ .

The response to  $152\text{-cm}^{-1}$  radiation was reduced in amplitude relative to the  $26.0\text{-cm}^{-1}$  response by approximately  $\frac{1}{25}$ . This reduction is close to a  $\sim 1/\omega^2$  dependence, i.e.,  $(\frac{26.0}{152})^2 \sim \frac{1}{32}$ . Such a dependence was also observed for granular NbN/BN, where it was interpreted as due to a response appropriate for  $\Omega \gg 1$  since, at  $87.7$  and  $152\text{-cm}^{-1}$ ,  $\hbar\omega \gg 2\Delta$ , where  $2\Delta \sim 35\text{-cm}^{-1}$  for NbN. Capacitive effects were not expected to dominate for this material because of the small intergrain capacitance (due to the  $\sim 100\text{-\AA}$  grain size). Our YBCO film, on the other hand, with grain sizes of  $\sim 0.1\text{--}1\text{ }\mu\text{m}$ , is expected to have larger intergrain capacitances, which will dominate the photoresponse at lower frequencies ( $\geq 30\text{-cm}^{-1}$ ) than expected for NbN/BN. At the same time the proposed (larger) superconducting gap of YBCO is about five times larger than the NbN gap. Only a weak confirmation for a remnant direct response at  $152\text{-cm}^{-1}$  was seen in the shift of the peaks of the photoresponse toward lower temperatures. More direct evidence for the (larger) superconducting energy gap of YBCO in the far-infrared photoresponse of granular films will only be possible with the availability of ultrathin, fine-grained films with the smallest possible intergrain capacitance.

## V. CONCLUSION

We have investigated the response of a granular film of  $\text{YBa}_{2.1}\text{Cu}_{3.4}\text{O}_{7-x}$  to radiation in the  $26\text{--}152\text{-cm}^{-1}$  spectral range. On the basis of the magnitude and dependence of the photoresponse on temperature, bias current, and far-infrared radiation intensity, we concluded that the  $26.0\text{-cm}^{-1}$  response was consistent with a model in which the far-infrared radiation directly modulates the intergrain Josephson currents. The magnitude of the photoresponse was proportional to the far-infrared power  $P$  for low power levels, but proportional to  $P^{1/2}$  for high power levels. The magnitude of the power at the crossover from a  $P$  to a  $P^{1/2}$  dependence was consistent with the proposed model. On the basis of analogous observations made previously for granular Sn films by Bertin and Rose,<sup>13</sup> interpreted in the context of the RSJ model, we concluded that the  $26.0\text{-cm}^{-1}$  photoresponse required that  $\hbar\omega \ll 2\Delta$ , where  $\hbar\omega = 26.0\text{-cm}^{-1}$  and  $2\Delta$  is the superconducting energy gap appropriate for our granular film. This conclusion precluded the possibility that a smaller gap ( $\sim 30\text{-cm}^{-1}$  or  $\sim 4\text{ meV}$ ), inferred from tunneling measurements, significantly affected the  $26.0\text{-cm}^{-1}$  photoresponse. The present experiment cannot address the validity of other proposed values for a smaller gap which fall in the  $12\text{--}19\text{ meV}$  range.

The above experiments have outlined a possible approach to investigate the photoresponse of granular films made from high-temperature superconductors. The measurements also demonstrate the need for low capacitance microstructures if the large superconducting gaps of the cuprate superconductors are to be displayed in a gap-dominated response to radiation in the  $100\text{--}500\text{ cm}^{-1}$  spectral range. The quasi-two-dimensional granular Nb-based films are excellent examples of granular films with very low intergranular capacitance. Current efforts are under way to realize similar films for the cuprates using two-target sputtering techniques. The resultant films

should provide a more controlled means of investigating large-gap, 2D granular superconductors.

#### ACKNOWLEDGMENTS

Helpful discussions with Mike Leung are acknowledged. We thank P. Skeath for growth of the film and Laura Allen for the SEM measurements. This research was supported in part by the Office of Naval Research. Work at the University of Florida was supported by NSF Grant No. DMR-9101676.

- <sup>1</sup>B. I. Halperin and D. R. Nelson, *J. Low Temp. Phys.* **36**, 599 (1979).
- <sup>2</sup>K. Epstein, A. M. Goldman, and A. M. Kadin, *Phys. Rev. Lett.* **47**, 534 (1981).
- <sup>3</sup>J. C. Culbertson, U. Strom, S. A. Wolf, and W. W. Fuller, *Phys. Rev. B* **44**, 9609 (1991).
- <sup>4</sup>P. L. Leath and W. Xia, *Phys. Rev. B* **44**, 9619 (1991).
- <sup>5</sup>A. M. Kadin, M. Leung, and A. D. Smith, *Phys. Rev. Lett.* **65**, 3193 (1990); A. M. Kadin, M. Leung, A. D. Smith, and J. M. Murdock, *Appl. Phys. Lett.* **57**, 2847 (1990); A. M. Kadin, *J. Appl. Phys.* **68**, 5741 (1990).
- <sup>6</sup>U. Strom, J. C. Culbertson, S. A. Wolf, S. Perkowitz, and G. L. Carr, *Phys. Rev. B* **42**, 4059 (1990).
- <sup>7</sup>D. U. Gubser, S. A. Wolf, W. W. Fuller, D. Van Vechten, and R. W. Simon, *Physica B* **135**, 131 (1985).
- <sup>8</sup>R. W. Simon, B. S. Dalrymple, D. Van Vechten, W. W. Fuller, and S. A. Wolf, *Phys. Rev. B* **36**, 1962 (1987).
- <sup>9</sup>Y. Enomoto and T. Murakami, *J. Appl. Phys.* **59**, 3807 (1986).
- <sup>10</sup>G. L. Carr, D. R. Kerecki, and S. Perkowitz, *J. Appl. Phys.* **55**, 3892 (1984).
- <sup>11</sup>P. G. Huggard, Gi. Schneider, T. O'Brian, P. Lemoine, W. Blau, and W. Prettl, *Appl. Phys. Lett.* **58**, 2549 (1991).
- <sup>12</sup>M. Leung, P. R. Broussard, J. H. Claassen, M. Osofsky, S. A. Wolf, and U. Strom, *Appl. Phys. Lett.* **51**, 2046 (1987).
- <sup>13</sup>F. Gao, G. L. Carr, C. D. Porter, D. B. Tanner, S. Etemad, T. Venkatesan, A. Inam, B. Dutta, X. D. Wu, G. P. Williams, and C. J. Hirschmugl, *Phys. Rev. B* **43**, 10383 (1991).
- <sup>14</sup>J. Orenstein, G. A. Thomas, A. J. Millis, S. L. Cooper, D. H. Rapkine, T. Timusk, L. F. Schneemeyer, and J. V. Waszak, *Phys. Rev. B* **42**, 6342 (1990).
- <sup>15</sup>K. Kamaras, S. L. Herr, C. D. Porter, N. Tache, D. B. Tanner, S. Etemad, T. Vankatesan, E. Chase, A. Inam, X. D. Wu, M. S. Hedge, and B. Dutta, *Phys. Rev. Lett.* **64**, 84 (1990).
- <sup>16</sup>C. L. Bertin and K. Rose, *J. Appl. Phys.* **39**, 2561 (1968).
- <sup>17</sup>C. L. Bertin and K. Rose, *J. Appl. Phys.* **42**, 631 (1971).
- <sup>18</sup>A. Barne and G. Paterno, *Physics and Applications of the Josephson Effect* (Wiley, New York, 1982), p. 305.
- <sup>19</sup>K. H. Lee, D. Stroud, and J. S. Chung, *Phys. Rev. Lett.* **64**, 962 (1990).
- <sup>20</sup>M. Tinkham, D. W. Abraham, and C. J. Lobb, *Phys. Rev. B* **26**, 6578 (1983).
- <sup>21</sup>D. C. Harris, S. T. Herbert, D. Stroud, and J. C. Garland, *Phys. Rev. Lett.* **67**, 3606 (1991).
- <sup>22</sup>W. J. Ayer, Jr. and K. Rose, *IEEE Trans. Magn.* **2**, 678 (1975).
- <sup>23</sup>E. T. Heyen, M. Cardona, J. Karpinski, E. Kaldis, and S. Rusiecki, *Phys. Rev. B* **43**, 12958 (1991).
- <sup>24</sup>M. Gurvitch, J. M. Valles, Jr., A. M. Cucolo, R. C. Dynes, J. P. Garno, L. F. Schneemeyer, and J. V. Waszczak, *Phys. Rev. Lett.* **63**, 1008 (1989).
- <sup>25</sup>Z. Schlesinger, R. T. Collins, F. Holtzberg, C. Feild, S. H. Blanton, U. Welp, G. W. Crabtree, Y. Fang, and J. Z. Liu, *Phys. Rev. Lett.* **65**, 801 (1990).
- <sup>26</sup>T. Pham, M. W. Lee, H. D. Drew, U. Welp, and Y. Fang, *Phys. Rev. B* **44**, 5377 (1991).
- <sup>27</sup>S. M. Anlage, B. W. Langley, G. Deutscher, J. Halbritter, and M. R. Beasley, *Phys. Rev. B* **44**, 9764 (1991).
- <sup>28</sup>V. Kresin and S. Wolf, *Phys. Rev. B* **41**, 4278 (1990).
- <sup>29</sup>M. R. Press and Sudhanshu S. Jha, *Phys. Rev. B* **44**, 300 (1991).